Langel SGT

NASA

Technical Memorandum 85012

(NASA-TM-85012) LARGE-SCALE, NEAR-EARTH, MAGNETIC FIELDS FROM EXTERNAL SOURCES AND THE CORRESPONDING INDUCED INTERNAL FIELD (NASA) 44 p HC A03/MF A01 CSCL 08E

N84-34807

Unclas
G3/46 24084

LARGE-SCALE, NEAR-EARTH, MAGNETIC FIELDS FROM EXTERNAL SOURCES AND THE CORRESPONDING INDUCED INTERNAL FIELD

R. A. Langel and R. H. Estes

APRIL 1983

National Aeronautics and
Space Administration

Goddard Space Flight Center
Greenbelt, Maryland 20771

LARGE-SCALE, NEAR-EARTH, MAGNETIC FIELDS FROM EXTERNAL SOURCES AND THE CORRESPONDING INDUCED INTERNAL FIELD

R.A. LANGEL[1]

AND

R.H. ESTES[2]

1. Geophysics Branch, Goddard Space Flight Center, Greenbelt, Md. 20771
2. Business and Technological Systems, Seabrook, Md. 20801

ABSTRACT

Magsat data has been analyzed as a function of the Dst index to determine the first degree/order spherical harmonic description of the near-earth external field and its corresponding induced field. The analysis was done separately for data from dawn and dusk with the following results:

Dusk external: $q_1^0 = 20.3 - 0.68$ Dst (nT)

Dusk internal: $g_1^0 = 29987.7 + 0.240\ q_1^0$ (nT)

Dawn external: $q_1^0 = 18.62 - 0.63$ Dst (nT)

Dawn internal: $g_1^0 = 29992.3 + 0.287\ q_1^0$ (nT)

Comparison with POGO data indicates that the constant term relating q_1^0 and Dst has changed about 20 nT between 1970 and 1980, presumably due to an increase in the average ring current intensity.

A local time variation of the external field persists even during very quiet magnetic conditions. Both a diurnal and 8-hour period are present. A crude estimate of Sq current in the 45^0 geomagnetic latitude range is obtained for 1966-1970. The current strength, located in the ionosphere and induced in the earth, is typical of earlier determinations from surface data, although its maximum is displaced in local time from previous results.

INTRODUCTION

Large scale current systems are known to exist on the boundaries of the magnetosphere, in the magnetotail and in an equatorial current sheet sometimes called the ring current. The fields from these current systems are likewise large scale and have been mapped throughout most of the magnetosphere and described as functions of the various magnetic activity indices and of local time (Fairfield, 1968,1971; Sugiura et al. 1971; Sugiura, 1972a,b; Sugiura and Poros, 1973, 1979; Hedgecock and Thomas, 1975) The equatorial current sheet is apparently the major contributor to these magnetic fields at and near the earth's surface. For purposes of this paper we cannot distinguish the various sources and will refer to the fields of interest as Large Scale External (LSE) fields. These are to be distinguished from more localized fields due to concentrations of current in "electrojets" or field aligned currents.

LSE fields are apparently always present. In magnetic observatory data their existence is inferred by study of the temporal variations they cause in the measured field. When analyzed on a global scale it becomes apparent that many of the observatory temporal variations can be described in terms of a systematic global morphology (e.g. Sugiura and Chapman, 1960), particularly during periods of significant magnetic activity. Typically, magnetically "quiet" days are selected and used to provide a "zero" level or base level from which to measure the temporal variation. If we designate the LSE fields by $\vec{D}$, then we can write:

$$\vec{D} = \vec{Dst} + \vec{DS} \qquad (1)$$

where $\vec{Dst}$ is the symmetric portion with respect to the earth's rotational axis and $\vec{DS}$ is the asymmetric portion. The horizontal component of Dst

at the equator is the commonly used "Dst index". There is some evidence (e.g. Langel and Sweeney, 1971) that DS can be very large during magnetic disturbances but tends to zero during quiet times. We doubt, however, that it actually goes to zero at any time. These definitions assume that DS is magnetospheric in origin, rather than ionospheric (see e.g. Cummings, 1966; Langel and Sweeney, 1971; Crooker and Siscoe, 1971), and that one can separate DS from the supposedly ionospheric daily variation , Sq. Averages of DS for selected classes of days (e.g. quiet, disturbed etc.) are often denoted by SD (see, e.g., Sugiura and Chapman, 1960).

It is clear that Dst and DS are relative quantities, i.e. their values depend upon the quiet level used to define "zero". The absolute magnitude of the LSE fields at and near the earth's surface has not previously been determined. Data from the recent Magsat mission is ideal for such a determination. The Magsat spacecraft (Langel et al., 1982) was launched on October 30, 1979, into a twilight, sun-synchronous orbit with inclination 96.76°, perigee 352 km and apogee 561 km. A Cesium vapor scalar and fluxgate vector magnetometer measured the field magnitude to better than 2 nanotesla (nT) and each component to better than 6 nT, r.s.s., including orbital and attitude determination errors. Magsat remained in orbit until June 11, 1980, although accurate vector data was obtained only until mid-May, 1980. Using two days of Magsat data, Langel et al. (1980) derived a global spherical harmonic model of the earth's main field, designated MGST(6/80), which included a solution for the lowest harmonic component of the LSE field. In particular, the external potential determined was of the form:

$$V_e = a(r/a)\{q_1^0 P_1^0(\theta) + [q_1^1\cos\phi + s_1^1\sin\phi]P_1^1(\theta)\} \qquad (2)$$

where r,θ,ϕ are the standard spherical coordinates, a is the mean radius of the earth, and P_n^m are Schmidt quasi-normalized Legendre functions. The coefficients determined were: q_1^0 = 20.4 nT, q_1^1 = -0.6 nT and s_1^1 = -0.4 nT. Previous studies (e.g. Chapman and Price, 1930; Rikitake and Sato, 1957; Langel and Sweeney, 1971) have indicated that most of the LSE field is represented by these first order terms. As noted by Langel et al. (1980), the equatorial value of the H component computed from the first order terms should closely represent the average absolute disturbance caused by LSE currents for the time period of the data. This in turn implies the ability to estimate an absolute baseline for Dst, at that time. For the period of data in MGST(6/80) the average Dst was 4.6, nT as compared with the average absolute value of equatorial H of -20.4 nT.

The present paper is an extension of the work of Langel et al. (1980). Magsat data has been analyzed for Dst between +20 nT and a relation between q_1^0 and Dst established. Because of the Magsat orbit, only twilight data is available. This was analyzed separately for dawn and dusk to take any local time asymmetry (i.e. DS) into account. Extrapolation to q_1^0 = 0 then enables us to estimate the true internal field from the core and the induced internal field from the time changing external fields. The analysis has proceeded in two ways, by spherical harmonic modeling of an appropriate Magsat data set and by analysis of individual Magsat passes. The two methods yield nearly the same results.

A re-analysis of magnetic field data from the POGO (Polar Orbiting Geophysical Observatories, OGO -2, -4, and -6, see e.g. Langel, 1974a) was carried out for comparison with the results from Magsat. The POGO data yielded less accurate results than the Magsat data since they

are field magnitude (scalar) data only. Some characteristics of the POGO satellites are presented in Table 1.

Table 1: Summary of POGO Satellite Characteristics.

SATELLITE	INCLINATION	PERIGEE	APOGEE	TIME PERIOD OF DATA USED
OGO -2	87.3°	410 km	1510 km	10/65 - 5/67
OGO -4	86.0°	410 km	910 km	8/67 - 1/69
OGO -6	82.0°	400 km	1100 km	6/69 - 8/70

The POGO data also yielded a relation between q_1^0 and Dst. Since this data covers all local times, the variation of that relation with local time was explored. Comparison with the Magsat results indicates that the zero level of Dst has changed about 20 nT between 1970 and 1980. The Sq current system is also apparent in the POGO data.

INITIAL DATA SELECTION FOR SPHERICAL HARMONIC ANALYSIS

We have begun with the assumption that Dst is a good indicator of relative changes in the LSE fields. Dr. M. Sugiura kindly furnished us the latest Dst values for the time period of the Magsat mission (November, 1979 through June, 1980). These values were derived from four observatories (Honolulu, San Juan, Hermanus and Kakioka) and contain final baseline adjustments. The Magsat data were then initially screened on the three hourly Kp index by choosing only data for Kp < 1- and for which the previous three hourly Kp index was <2o. Component data at latitudes poleward of 50° geomagnetic latitude was excluded to minimize the effects

of field aligned and ionospheric currents in the auroral regions, while scalar data were retained. After the initial screening, the data was sorted into separate subsets for dawn and dusk, according to the Dst value at the time of the measurement, and visually scanned both for quality and to assure minimization of the effects of short wavelength external fields. Table 2 is a tabulation by Dst range of the number of data points available for each Dst range and an evaluation of their geographical coverage. The geographical coverage from most of these data sets is far from satisfactory and, as will be seen, this has an adverse effect on some of the analysis.

SPHERICAL HARMONIC ANALYSIS BY Dst LEVEL

Twelve of the eighteen subsets of data described in Table 2 were utilized to derive spherical harmonic expansions of degree and order thirteen in constant coefficients, seven in the first time derivative coefficients, and one in external terms. Table 3 summarizes some of the results from these models.

To begin we focused on the relationship between Dst and q_1^0. This is plotted, for both dawn and dusk, in Figure 1. The relationship is clearly linear over the range of Dst considered. Regression analyses give:

$$q_1^0 = 19.8 - 0.63 \text{ Dst}, \quad \text{nT}, \quad \text{Dusk} \qquad (3a)$$

$$q_1^0 = 18.1 - 0.55 \text{ Dst}, \quad \text{nT}, \quad \text{Dawn} \qquad (3b)$$

with an rms of 0.54 nT and 0.52 nT, respectively.

The LSE fields vary with time and cause induced currents within the earth which, in turn, give rise to internal fields. Presumably the mean of such fields, for magnetically quiet times, is absorbed into the g_1^0 internal term of standard spherical harmonic analyses of the main field.

To attempt to isolate this induced component of internal field from the field originating in the core, we examined the relationship between q_1^0 and g_1^0, as tabulated in Table 3. Figure 2 is a plot of these variables. Clearly the scatter in the determination of q_1^0 is large. If, however, we ignore the three circled points, a trend is evident. Regression analyses of the remaining points give:

$$g_1^0 = -29991.7 + 0.56q_1^0 \quad \text{nT}, \quad \text{Dusk} \qquad (4a)$$

$$g_1^0 = -29990.9 + 0.35q_1^0 \quad \text{nT}, \quad \text{Dawn} \qquad (4b)$$

with rms of 1.25 nT and 0.52 nT, respectively. The circled points are for Dst = -10 and 15 nT (Dawn) and Dst = 15 nT (Dusk). From Table 2, two of these data distributions are bad and the other is poor, so we feel justified in excluding them from the analysis. It is, perhaps, surprising that the corresponding q_1^0 values are in such good agreement with the other values of Figure 1. One possible explanation is that a poor geographic distribution of data implies an even poorer temporal distribution, and the secular variation terms are more highly correlated with the constant internal terms than with the constant external terms. This could result in larger errors in g_1^0 than in q_1^0 for the same model.

We are not certain how to assign error bars to the data in either Figure 1 or Figure 2. The standard errors computed in the least squares modeling procedure are, in most cases, less than 0.5 nT, but we believe this underestimates the actual error. As a rule of thumb we feel that, for Dst levels with adequate geographic distribution, q_1^0 and g_1^0 are probably accurate to ±2 nT.

COMBINED SPHERICAL HARMONIC ANALYSIS

In order to verify the results of the previous section and to attempt to improve the accuracy of (3) and (4), the spherical harmonic analysis software was modified to permit a direct solution for (3) and (4) using a data set selected from all of the Dst levels.

The data selection algorithm was applied separately for the time intervals (1) November - December, 1979, (2) January - February, 1980, and, (3), March - April, 1980, in an attempt to obtain a uniform data distribution in both time and space. For each period, and for dawn and dusk separately, vector data within $\pm 50^{\circ}$ geomagnetic latitude and magnitude data poleward of $\pm 50^{\circ}$ geomagnetic latitude were collected into 5° by 5° equiangular bins over the globe. In regions where vector data were sparse within $\pm 50^{\circ}$, available scalar data were retained. Within each bin the data was sorted by time and a mean and standard deviation calculated. All data with residual (relative to the GSFC(9/80) model, Langel et al., 1982) greater than 150 nT, and/or greater than 2σ from the mean, is rejected. The desired number of points in each bin was selected so as to obtain roughly the same number of points for equal area at all latitudes. This was accomplished by specifying a maximum of nine values for each vector component in an equatorial $5^{\circ}x5^{\circ}$ bin, and scaling the number of points in each bin at other latitudes by the cosine of the latitude. An equatorial bin value of twenty seven was used for scalar data to be retained poleward of $\pm 50^{\circ}$, while six was used for scalar data retained within $\pm 50^{\circ}$. Each of the nine

Dst intervals was assigned a weight (in nT) as follows:

Dst	-20	-15	-10	-5	0	5	10	15	20
Weight	8	8	8	8	8	10	12	14	16

If a bin has more data than is desired after applying the above criteria, data is rejected first by an interval skipping algorithm (to maintain good temporal distribution) and then by eliminating data with higher weights. A computer error resulted in a less than proportionate selection from the Dst = -15nT data interval, but the final data sets, dawn and dusk, both have adequate temporal and geographic distributions. The mean and sigma of the residuals for each data type within each bin for the resulting global distribution was computed. To obtain a managable data set for least squares modeling while retaining good temporal and geographic coverage, the above global data sets were reduced to approximately one third size. Within each $5^0 \times 5^0$ bin, and for each data type, an interval skipping algorithm was used (with data sorted by time) to take every third point. Any further reduction required was accomplished by eliminating that data with the largest absolute deviation from the mean within the bin. The data distribution of the resulting global data sets, which are used in the combined spherical harmonic analysis, are presented in Table 4 by Dst interval.

The spherical harmonic analyses for dawn and dusk using the combined data sets from all Dst levels yielded the following results:

$$q_1^0 = 18.62 - 0.63\ \mathrm{Dst} \quad \text{nT, Dawn} \qquad (5a)$$

$$q_1^0 = 20.30 - 0.68\ \mathrm{Dst} \quad \text{nT, Dusk} \qquad (5b)$$

$$g_1^0 = -29992.3 + 0.29 q_1^0 \quad \text{nT, Dawn} \qquad (6a)$$

$$g_1^0 = -29987.7 + 0.24 q_1^0 \quad \text{nT, Dusk} \qquad (6b)$$

These are to be compared with equations (3) and (4) respectively. We

consider the agreement to be quite good, and because the data distribution is better for equations (5) and (6) we consider these to be more accurate than (3) and (4). The difference in the constant term between (6a) and (6b) was unexpected and will be addressed in another paper in preparation.

ANALYSIS OF INDIVIDUAL PASSES

The residual field after subtraction of a core field model (spherical harmonic analysis) from the measured data, e.g.

$$\Delta\vec{B} = \vec{B}(\text{measured}) - \vec{B}(\text{computed}) \qquad (7a)$$

$$\Delta B = |\vec{B}(\text{measured})| - |\vec{B}(\text{computed})| \qquad (7b)$$

is due to (i) fields from external currents and the corresponding induced currents, (ii) crustal anomalies and, (iii), measurement and field model errors. We will assume that (iii) is negligible. At low latitudes, away from noon, the external portion of (7) is dominated by the long-wavelength LSE fields. We also assume that (ii) is negligible at these wavelengths, and that (i) is described by a potential field of the form (Chapman and Price, 1930; Rikitake and Sato, 1957):

$$V = a\,[(r/a)e + (a/r)^2 i)]\cos\theta \qquad (8)$$

where r is geocentric radius, θ is geomagnetic latitude and "a" is the mean radius of the earth. Here e corresponds to q_1^0 in (2), except one uses geographic and the other geomagnetic latitude. Langel and Sweeney (1971) and Langel (1974b) showed that a pass of satellite data between $\pm 45^0$ latitude was sufficient to solve for e and i in a least squares sense, even if only scalar data is available. Such a solution is more accurate when component data is available, as from Magsat.

We have computed e and i for all Magsat passes, both from the vector and from the scalar data. The residual fields used were relative to the MGST(4/81) spherical harmonic model. This model is of degree and order thirteen in constant terms and seven in first time derivative terms. Though unpublished, MGST(4/81) may be obtained from the authors.

Figures 3 and 4 show e plotted versus Dst for dawn and dusk. The range of Dst is limited to ±20 nT; there are 1211 points at dawn and 1163 points at dusk. Regression lines fit to the data give:

$$e = 21.3 - 0.62\ Dst \quad nT, \quad Dawn \qquad (9a)$$

$$e = 22.4 - 0.72\ Dst \quad nT, \quad Dusk \qquad (9b)$$

with standard deviations of 3.9 nT and 4.2 nT, respectively, and correlation coefficients of 0.82 and 0.85, respectively.

Figures 5 and 6 show i plotted verses e. Regression lines fit to the data give:

$$i = -6.1 + 0.17e \quad nT, \quad Dawn \qquad (10a)$$

$$i = 0.3 + 0.21e \quad nT, \quad Dusk \qquad (10b)$$

with standard deviations of 3.6 nT and 3.8 nT and correlation coefficients of 0.31 and 0.39, respectively.

Equations (9) are in very good agreement with equations (3) and (5) and so we are confident we have established a clear relationship between q_1^0 and Dst for the epoch of the Magsat data.

The relationship between i and e is less satisfactory, although the slopes in (10) are certainly consistent with those in (4) and (6). We had expected the correlation coefficients to be larger and the scatter in Figures 5 and 6 to be less. Theoretically, the i/e ratio will depend upon the rate of change of e and we thought that taking this into account might improve the results. However, a plot of i/e as a function of the

rate of change of e showed no correlation. The computed correlation coefficient was 0.06.

Another difficulty with (10) arises from the field model, MGST(4/81), used to reduce the data. No account was taken of the external or induced fields in deriving this model. The effect of this on the determination of e and i is not known, but clearly the g_1^0 term in the MGST(4/81) model will have absorbed some of the induced fields so that the constant terms in (10) are somewhat uncertain.

ANALYSIS OF POGO DATA

The POGO data are scalar field measurements only. Attempts to solve for external fields with spherical harmonic analysis using this data have been inconclusive. However, analysis of individual passes to solve for the coefficients e and i in (10) is possible (Langel, 1974b). To carry out this analysis the POGO data were subdivided into Dst bins 5nT wide centered at 5 nT intervals between ±20 nT, into local time bins 2 hours wide centered at 0, 2, 4,...22 hours, and into geomagnetic latitude bins 5^0 wide centered at even 5^0 intervals between ±40^0. The residuals relative to the POGO(8/71) spherical harmonic model (Langel, 1974a) were averaged within each bin. Solutions for e and i were then obtained for each Dst and local time. For each local time a regression analysis of the form:

$$e = a + b\ Dst \qquad (11)$$

and

$$i = c + d\ e \qquad (12)$$

was computed. Table 5 gives the values of a, b, c and d for each local time; Figures 7 and 8 contain the corresponding plots. Notice that the zero hour value is present on both ends of the plot. A local time variation is present in a, b and c, but we regard d to be constant at its average value, 0.22, to within the accuracy of our determination. The local time dependance of a and b is clearly of a sinusoidal nature. Fourier analysis yields:

$$a = 0.40 - 2.87\sin(t-8.2^0) + 1.82\sin(3t+12.05^0),\ nT \qquad (13)$$

$$b = -0.680 + 0.134\sin(t+13^0) \qquad (14)$$

where t is the local time in degrees. Calculated values from equations 13 and 14 are given as solid lines in Figure 7.

A diurnal variation of Ds was found by Sugiura and Chapman (1960), who also found significant semi-diurnal variation. To our knowledge the period of 8 hours has not been seen previously in fields originating external to the ionosphere. Although small, we see no reason at present to doubt its reality. The absence of the 8 hour period in b means that its magnitude is essentially constant regardless of Dst level, for Dst within 20 nT. This seems to suggest that its origin lies in magnetopause currents rather than the ring current.

The semi-diurnal terms in the Fourier analysis were:

$$a\ (\text{semi-diurnal}) = 0.72\sin(2t + 53^0) \qquad (15a)$$

$$b\ (\text{semi-diurnal}) = 0.23\sin(2t + 105^0) \qquad (15b)$$

However the spectral power density of the semi-diurnal term for a is a factor of seven down from the 8 hour period and for b it is a factor of 35 down from the diurnal term. We do not regard these terms as significant, although their amplitudes, relative to the diurnal coefficients in (13) and (14), are comparable to those found by Sugiura and Chapman (1960).

It is apparent that the local time variations persist at all Dst levels and that the strength of the diurnal variation, in particular, grows as Dst becomes more negative. It should be kept in mind that the present anaylsis considers data averaged over Dst. The results, therefore, indicate the variation fields averaged over both Dst and time and are thus unable to distinguish the variations of a and b over short periods of time. That such variations exist has been shown clearly by Crooker (1972).

The potential

$$V = a\,(a/r)^2\, i \cos\theta \qquad (16)$$

describes fields originating internal to the satellite altitude. Such fields may be of two origins: from currents in the ionosphere or from currents induced in the earth. If

$$i = i_m + i_s, \qquad (17)$$

where i_m represents fields induced by currents in the magnetosphere and i_s represents ionospheric currents and their corresponding induced earth currents, (presumably Sq for these Dst levels), then:

$$i_m + i_s = c + d\,e. \qquad (18)$$

If the external field, e, goes to zero i_m should also go to zero from which we infer that c is strictly associated with Sq. It would be nice if we could say that d is strictly associated with earth currents induced by magnetospheric currents, as is perhaps likely, but that cannot be concluded with certainty. Any portion of Sq which varies with Dst will also be included in d.

Under the assumption that contributions of Sq to d are small, we can substitute c for i in equation (16) to obtain the potential for Sq. There is a zero-level uncertainty to this procedure because some portion of the Sq field will have been absorbed into the spherical harmonic model used to represent the core field. Table 5 gives the coefficients of this potential for each of twelve local times. These potentials are approximations since they are derived using data only between ±40° geomagnetic latitude along a single local time meridian, and assume a strictly $P_1^0(\cos\theta)$ functional relationship. This procedure does not yield a

global potential. It is possible, however, to compute a current function, ψ, along each of the local time meridians, between 45^{o} latitude. Under the assumption of zero current near midnight, we have added 2.0 to the values of Table 5 when performing this calculation.

The resulting current is shown in Figure 9. Coordinates are geomagnetic latitude and solar local time. Comparison with typical Sq current systems derived from observatory data indicates good agreement in current direction and magnitude. Those systems, however, indicate that the current maximum should occur near 1100 hours wheras the maximum current in Figure 9 occurs near 1300 hours. We are unable to account for the discrepancy at this time.

Mead (1964) and Olson(e.g. 1970) have pointed out that the LSE fields at the earth contain variations similar to the Sq field. This has raised the question , still unresolved, as to how much of the Sq field originates in ionospheric currents and how much originates external to the ionosphere. The equivalent current system of Figure 9 must reside in the ionosphere and the earth itself, at least to within the accuracy of our determination. This would indicate that the major part of Sq is ionospheric in origin, although it does not exclude a magnetospheric contribution.

COMPARISON OF MAGSAT AND POGO RESULTS

Writing

$$q_1^0 = a + b\ Dst \qquad (19a)$$

$$i = d\ q_1^0, \qquad (19b)$$

a summary of results for dawn and dusk is given in Table 6. Comparing Magsat and POGO shows that the asymmetry between dawn and dusk is present in both data sets. The values of d from POGO are identical with the Magsat values from the combined spherical harmonic analysis, which we regard as the most accurate Magsat determination. Variation of b is larger in the POGO results than in Magsat and the values of a are significantly different.

The most important difference is that in the value of a. Magsat data yields a value 23.1 nT higher than POGO data at dawn and 15.6 nT higher at dusk. Thus, from (19a), for the same level of Dst the magnitude of the external field near the earth is about 20 nT higher at 1980 than during 1966-1970. This difference seems somewhat excessive. The question arose as to whether use of the POGO(8/71) spherical harmonic model to reduce the POGO data might be introducing a bias since it is only of degree/order ten. Accordingly, a portion of the POGO analysis was redone using the GSFC(9/80) model (Langel et al., 1982). No significant change in the a or b coefficients was found. The data in both these models for the 1966-1970 time period is predominantly scalar (from POGO), which still leaves some question as to how accurate a model is obtainable. However, we have no indication that the models could be in error by as much as 20 nT.

Assuming the calculation to be correct, we are led to conclude that

either the definition of the Dst baseline has changed or that the sources of the external field have changed. The baseline for Dst is derived from selected magnetically quiet days, after removing effects from Sq. The method of analysis has been self consistent for a period of time exceeding that under discussion here (Sugiura, private communication). We see no reason to attribute any change to its definition. On the other hand, magnetic quiet is defined in terms of the temporal variation of the field at the various observatories, and a long-term change in external fields might not be detectable as such in surface data but could very well appear to be part of the main field secular variation.

Let us assume that the external sources have changed. As seen from near the earth these external fields may be considered to be the result of two competing mechanisms. The ring current and tail current, or equatorial current sheet, inflates the magnetosphere. An increase in the average level of these currents would result in an increase in the value of the coefficient a. Compression of the magnetosphere by increased solar wind pressure (an increase in magnetopause currents) would result in a decrease of the coefficient a. Between 1966-1970 (POGO epoch) and 1980 (Magsat epoch) we observe the coefficient a increasing by about 20 nT which implies increased inflation of the magnetosphere or decreased magnetopause compression. In fact, on average, the magnetopause compression increased. From Mead (1964) we find that the field at the earth from Magnetopause compression increases by about 7.5 nT for each earth radius of contraction of the radius of the subsolar magnetopause. It is commonly accepted that the subsolar magnetopause varies inversly with the sixth

power of solar wind pressure. The average solar wind pressure for the POGO epoch was 1.54×10^{-8} dynes/cc and for the Magsat epoch 2.3×10^{-8} dynes/cc (J. King, private communication). Thus the magnetopause radius, on average, was less during the Magsat period than the POGO period. A simple calculation shows that the field at the earth would have decreased (or the coefficient, a, would have increased) by a little over 5 nT.

This implies that the amount of inflation of the magnetosphere due to the ring and tail currents was greater in 1980 than in 1966-1970.

The four year period of the POGO data is considerably longer than the 7.5 months of Magsat data. To determine if the coefficients a and b changed during 1966-1970, the POGO data was subdivided into nine time intervals and separate analysis made. No apparent change in the coefficients was found.

SUMMARY AND DISCUSSION

Estimates of the magnitude and temporal variation of the near-earth LSE fields have been available for some time. Magnetospheric models have been designed to represent the magnetic field throughout the entire magnetosphere, of which the vicinity of the earth is a very small part. Further, the fields of interest in those models are very weak near the earth so that even small model shortcomings can result in a large percentage error in representing the near-earth field (Olson and Pfitzer, 1981). Complicating the issue further is the difficulty inherent in attempting to isolate the external fields from the internal fields near the earth. Observatory data has been used successfully to show that most of the Sq fields are external to the earth and the most plausible theories regarding origin of the Sq field indicated currents in the ionosphere. Now, however, we find (Olson, 1970) that a portion of Sq may be magnetospheric in origin. Plausible arguments were made from observatory data that, at least during magnetic storms, the symmetric part of D (Dst) originated in a ring current external to the ionosphere. Ds fields were originally analyzed in terms of ionospheric currents (e.g. Chapman, 1935). Later it was argued that at least some of DS was magnetospheric rather than ionospheric (e.g. Akasofu and Chapman, 1964). However definitive separation between ionospheric and magnetospheric sources requires data at altitudes between the two, i.e. from a satellite (e.g. Langel and Sweeney, 1971) and, where possible, data in the actual current region (e.g. Sugiura, 1972b). Study of LSE fields with observatory data has focused on the time-varying portion of those fields, especially during magnetic storms. From measurements at the earth's surface it has not

been possible to describe LSE fields which may be nearly constant in time. Field variations which correlate with solar activity have been found(Yukutake, 1965; Alldredge, 1976; Sugiura, 1976; Harwood and Malin, 1977; Sugiura and Poros, 1977; Alldredge et al., 1979; Yukutake and Cain, 1979) and attributed to external fields, although their isolation is extremely difficult and the accuracy with which the determination is made is problematical.

We have derived a description of the average LSE field and the corresponding induced field between 45° geomagnetic latitude for magnetically quiet periods in terms of a first degree/order spherical harmonic analysis of Magsat data. This model relates the LSE field directly with the Dst index, establishing an absolute baseline for Dst at 1980. Separate analyses for dawn and dusk local times showed a distinct asymmetry. This was confirmed by an analysis of POGO data from 1966-1970 in which the asymmetry was found to have both an 8 and a 24 hour variation with local time. The amplitude of the local time variation was greater in the POGO data than in the Magsat data, even though the Dst levels were the same. Both sets of data show that the amplitude of the asymmetry increases as Dst becomes more negative. Thus, although the external field asymmetry is greater during magnetic storms, it never entirely disappears. We are unable to tell if this is because the ring-current never becomes completely symmetric or if the source of the asymmetry lies in magnetopause and magnetotail currents.

Previously Langel et al. (1980) found q_1^0 to be 20.4 nT for provisional Dst ≈ 4.6 nT. The adjusted Dst for the epoch of that analysis is 3 nT. From (5) we now predict q_1^0 to be 16.7 nT at dawn and 18.3 nT at dusk, or about 2-4 nT lower than the earlier result. The statement by Langel et

al. (1980), "To estimate the longitudinally symmetric portion of the disturbance one should subtract 25 nT from the value of Dst..." is incorrect. Equations (5) and (6) give the correct estimate.

Comparison of POGO and Magsat results indicates an increase in the average quiet-time intensity of the LSE fields from 1966-1970 to 1980, which must be attributed to an intensification of the ring current. The magnitude of the change is about 20 nT. Because the POGO analysis is dependant on scalar data only, it is difficult to estimate the accuracy of this result. However, comparison of similar calculations from Magsat showed that separation of the internal and external fields on individual passes using only scalar data was usually within 4 nT of the separation using only vector data.

Sq fields have also been shown to be discernable in the POGO data. To the accuracy of our determination, these arise entirely internal to the spacecraft altitude, suggesting that any contributions to Sq from LSE fields is small.

Finally, the magnitude of the coefficient of P_1^0 for induced fields is about 0.24 to 0.29 of the corresponding coefficient for the inducing field. This has implications for the investigation of upper mantle conductivity as already studied for the POGO data by Langel (1974b) and, more extensively, by Didwall (1981).

TABLE 2: DATA DISTRIBUTION FOR EACH DST INTERVAL

	DAWN			DUSK		
Dst(nT 2.5)	Scalar	Vector*	Geographic Coverage	Scalar	Vector*	Geographic Coverage
20	298	588	Very bad	310	547	Very bad
15	679	1511	Bad	654	1111	Bad
10	2340	3619	Fair	2595	3481	Fair
5	2566	5298	Fair	2761	4715	Good
0	2615	6120	Good	2541	5819	Good
-5	2242	4344	Fair	1823	3865	Fair
-10	884	2128	Poor	1089	2337	Poor
-15	378	859	Bad	340	784	Bad
-20	349	670	Bad	552	883	Bad

* Only vector data between $\pm 50^0$ geographic latitude was included in spherical harmonic least squares fits for the separate Dst intervals.

TABLE 3: PARAMETERS FROM SPHERICAL HARMONIC MODELS BY Dst, ALL UNITS ARE nT.

D A W N

Dst	g_1^0(external)	g_1^0(internal, core plus induced)
15	10.1	-29968.9
10	12.2	-29986.3
5	15.1	-29986.3
0	17.9	-29984.9
-5	21.9	-29982.6
-10	23.1	-29971.7

D U S K

15	9.5	-29941.9
10	14.3	-29983.2
5	16.4	-29982.0
0	20.2	-29982.1
-5	23.3	-29979.8
-10	25.5	-29975.7

TABLE 4: DISTRIBUTION OF DATA BY Dst INTERVAL IN COMBINED DATA SETS

	D A W N		D U S K	
	Number of points		Number of points	
Dst(nT, 2.5)	Scalar	Vector	Scalar	Vector
20	143	48	157	85
15	436	260	427	240
10	1739	1030	1886	1120
5	2471	1985	2492	1960
0	3242	2790	3192	2780
-5	2447	1875	2110	1735
-10	1070	900	1194	945
-15	39	15	43	25
-20	401	300	560	440

TABLE 5: REGRESSION COEFICIENTS FROM POGO DATA BY LOCAL TIME

Coefficient	LOCAL TIME											
	0	2	4	6	8	10	12	14	16	18	20	22
a (nT)[1]	1.8	1.9	-2.5	-4.5	-2.4	-0.4	1.2	-0.4	3.3	4.7	1.7	0.4
b[1]	-0.66	-0.57	-0.50	-0.57	-0.61	-0.65	-0.75	-0.76	-0.75	-0.84	-0.77	-0.77
c (nT)[2]	-2.2	-2.8	-1.6	-1.1	-0.5	2.8	8.5	9.1	3.6	0.0	0.2	-1.7
d[2]	0.11	0.21	0.23	0.29	0.23	0.29	0.27	0.27	0.18	0.24	0.16	0.17
$\sigma 1^1$	0.4	0.8	0.9	0.3	1.1	1.1	0.7	0.6	1.1	0.7	0.4	1.0
$\sigma 2^2$	0.3	0.3	1.0	0.3	0.5	0.7	0.4	0.6	1.0	0.5	0.5	0.5

1 Coefficients and standard deviations of data for equation (11)

2 Coefficients and standard deviations of data for equation (12)

TABLE 6: SUMMARY OF RESULTS

	DAWN			DUSK		
	a	b	d	a	b	d
Magsat: Combined Spherical Harmonic Analysis	18.6	-0.63	0.29	20.3	-0.68	0.24
Individual Spherical Harmonic Analysis	18.1	-0.55	0.35	19.8	-0.63	0.56
Individual Passes	21.3	-0.62	0.17	22.4	-0.72	0.21
POGO: Individual Passes	-4.5	-0.57	0.29	4.7	-0.84	0.24

ACKNOWLEDGEMENTS

The authors wish to thank J. King for supplying solar wind pressure data, and M. Sugiura for supplying Dst data. Some of the computational effort was performed by Kevin Coakley, Jim Richardson, Stuart Goldman and Tom Podles. We appreciate the support of Magsat project personnel at Nasa Headquarters, particularly Tom Fischetti, James Murphy and Mark Settle.

Figure Captions

Figure 1: First degree/order coefficient of the external potential, q_1^0, as a function of the Dst index for dawn and dusk local times. Each coefficient q_1^0 was determined in a spherical harmonic analysis of the main and external fields in which all data was from periods of time when Dst was within 2.5 nT of its nominal value.

Figure 2: First degree/order coefficient of the internal coefficient, q_1^0, as a function of the first degree/order external coefficient, q_1^0. Each determination uses data for which Dst was confined to a ±2.5 nT range, as described in the caption to Figure 1.

Figure 3: First degree/order coefficient, e, of the external potential fit to the X and Z component residual fields from individual Magsat passes verses the Dst index at the time of the equator crossing of that pass. Data are for dawn local time only.

Figure 4: Same as Figure 3 except dusk local time only.

Figure 5: First degree/order coefficient, i, of the internal field versus first degree/order coefficient, e, of the external field as determined from the X and Z component residual fields from individual Magsat passes. Data are for dawn local time only.

Figure 6: Same as Figure 5 except dusk local time only.

Figure 7: Local time variation of coefficients a and b from equation (11) describing the external field for POGO data as a function of Dst.

Figure 8: Local time variation of coefficients c and d from equation (12) describing the internal disturbance field potential for POGO data as a function of Dst.

Figure 9: Equivalent current system corresponding to the disturbance field internal to the POGO orbit and extrapolated to the condition of zero field from magnetospheric sources. 2.5×10^4 Amps. flows between streamlines.

REFERENCES

Akasofu, S.-I., and S. Chapman, On the asymmetric development of magnetic storm fields in low and middle latitudes, Planet. Space. Sci., 12, 607-626, 1964

Alldredge, L.R., Effects of solar activity on annual means of geomagnetic components, Jour. Geophys. Res., 81, 2990-2996, 1976

Alldredge, L.R., C.O. Stearns and M. Sugiura, The determination of geomagnetic external spherical harmonic coefficients, J. Geomag. Geoelectr., 31, 495-508, 1979

Cummings, W.D., Asymmetric ring currents and the low-latitude disturbance daily variation, Jour. Geophys. Res., 71, 4495-4503, 1966

Chapman, S., The electric current systems of magnetic storms, Terr. Magn. Atmos. Elec., 40, 349, 1935

Chapman, S. and A.T. Price, The electric and magnetic state of the interior of the earth as inferred from terrestrial magnetic variations, Phil. Trans. Roy. Soc. London, A, 229, 427-460, 1930

Crooker, N.U., High-time resolution of the low-latitude asymmetric disturbance in the geomagnetic field, Jour. Geophys. Res., 77, 773-775, 1972

Crooker, N.U. and G.L. Siscoe, A study of the geomagnetic disturbance asymmetry, Radio Sci., 6, 495-501, 1971

Fairfield, D.H., Average magnetic field configuration of the outer magnetosphere, Jour. Geophys. Res., 73, 7329, 1968

Fairfield, D.H., Average and unusual locations of the earth's magnetopause and bowshock, Jour. Geophys. Res., 76, 6700, 1971

Fairfield, D.H., On the average configuration of the geomagnetic tail, Jour. Geophys. Res., 84, 1950, 1979

Harwood, J.M., and S.R.C. Malin, Sunspon cycle influence on the geomagnetic field, Geophys. J. R. astr. Soc., 50, 605-619, 1977

Hedgecock, P.C. and B.T. Thomas, HEOS observations of the configuration of the magnetosphere, Geophys. J. R. astr Soc., 41, 391, 1975

Langel, R.A., Near-earth magnetic disturbance in total field at high latitudes, 1. Summary of data from OGO 2, 4 and 6, Jour. Geophys. Res., 79, 2363, 1974a

Langel, R.A., Induced fields as measured by the OGO 2, 4 and 6 spacecraft, Second Workshop on Electromagnetic Induction in the Earth, (IUGG and IAGA), Ottawa Canada, Abs. 1974b

Langel, R.A. and R.E. Sweeney, Asymmetric ring current at twilight local time, Jour. Geophys. Res., 76, 4420, 1971

Langel, R., R.H. Estes, G.D. Mead, E.B. Fabiano and E.R. Lancaster, Initial geomagnetic field model from Magsat vector data, Geophys. Res. Lettr., 7, 793-796, 1980

Langel, R.A., G. Ousley, J. Berbert, J. Murphy and M. Settle, The Magsat mission, Geophys. Res. Lettr., 9, 243, 1982a

Langel, R.A., R.H. Estes and G.D. Mead, Some new methods in geomagnetic field modeling applied to the 1960-1980 epoch, Jour. Geomag. Geoelec., 34, 327-349, 1982

Mead, G.D., Deformation of the geomagnetic field by the solar wind, Jour. Geophys. Res., 69, 1181, 1964

Olson, W.P., Contribution of nonionospheric currents to the quiet daily magnetic variations at the earth's surface, Jour. Geophys. Res., 75, 7244-7249, 1970

Olson, W.P. and K.A. Pfitzer, The accurate determination of the magnetospheric magnetic field in the vicinity of the earth, (Abstract) 4th IAGA Scientific Assembly, Edinburgh, IAGA Bulleton No.45, IUGG Publications Office, 39 Rue Gay Lussac, Paris, 75005, France, 1981

Rikitake, T. and S. Sato, The geomagnetic Dst field of the magnetic storm on June 18-19, 1936, Bull. Earthquake Res. Inst., Tokyo Univ., 35, 7-21, 1957

Sugiura, M., Equatorial current sheet in the magnetosphere, Jour. Geophys. Res., 77, 6093, 1972a

Sugiura, M., The ring current, in Critical Problems of Magnetospheric Physics, ed. E.R. Dyer, pp 195-210, Inter-Union Commission on Solar-Terrestrial Physics, c/o National Academy of Sciences, Washington, D.C., 1972b

Sugiura, M., and S. Chapman, The average morphology of geomagnetic storms with sudden commencement, Abh. Akad. Wiss. Gottingen, Math.-Phys. Kl., Sonderheft, no4, 1960

Sugiura, M., B.G. Ledley, T.L. Skillman and J.P. Heppner, Magnetospheric field distortions observed by Ogo 3 and 5, Jour. Geophys. Res., 76, 7552-7565, 1971

Sugiura, M. and D.J. Poros, A magnetospheric field model incorporating the Ogo-3 and 5 magnetic field observations, Planet. Space Sci., 21, 1763, 1973

Sugiura, M., Quasi-biennial geomagnetic variation caused by the sun, Geophys. Res. Lettr., 3, 643, 1976

Sugiura, M. and D.J. Poros, Solar generated quasi-biennial geomagnetic variation, Jour. Geophys. Res., 82, 5621, 1977

Sugiura, M., and D.J. Poros, A method of evaluating quantitative magnetospheric field models by an angular parameter ω, in Quantitative Modeling of Magnetospheric Processes, W.P. Olson (ed.), pg 48-63, American Geophysical Union, Washington D.C., 1979

Yukutake, T., The solar cycle contribution to the secular change in the geomagnetic field, Jour. Geomag. Geoelec., 17, 287-309, 1965

Yukutake, T. and J.C. Cain, Solar cycle variations of the first-degree spherical harmonic components of the geomagnetic field, Jour. Geomag. Geoelec., 31, 509-544, 1979

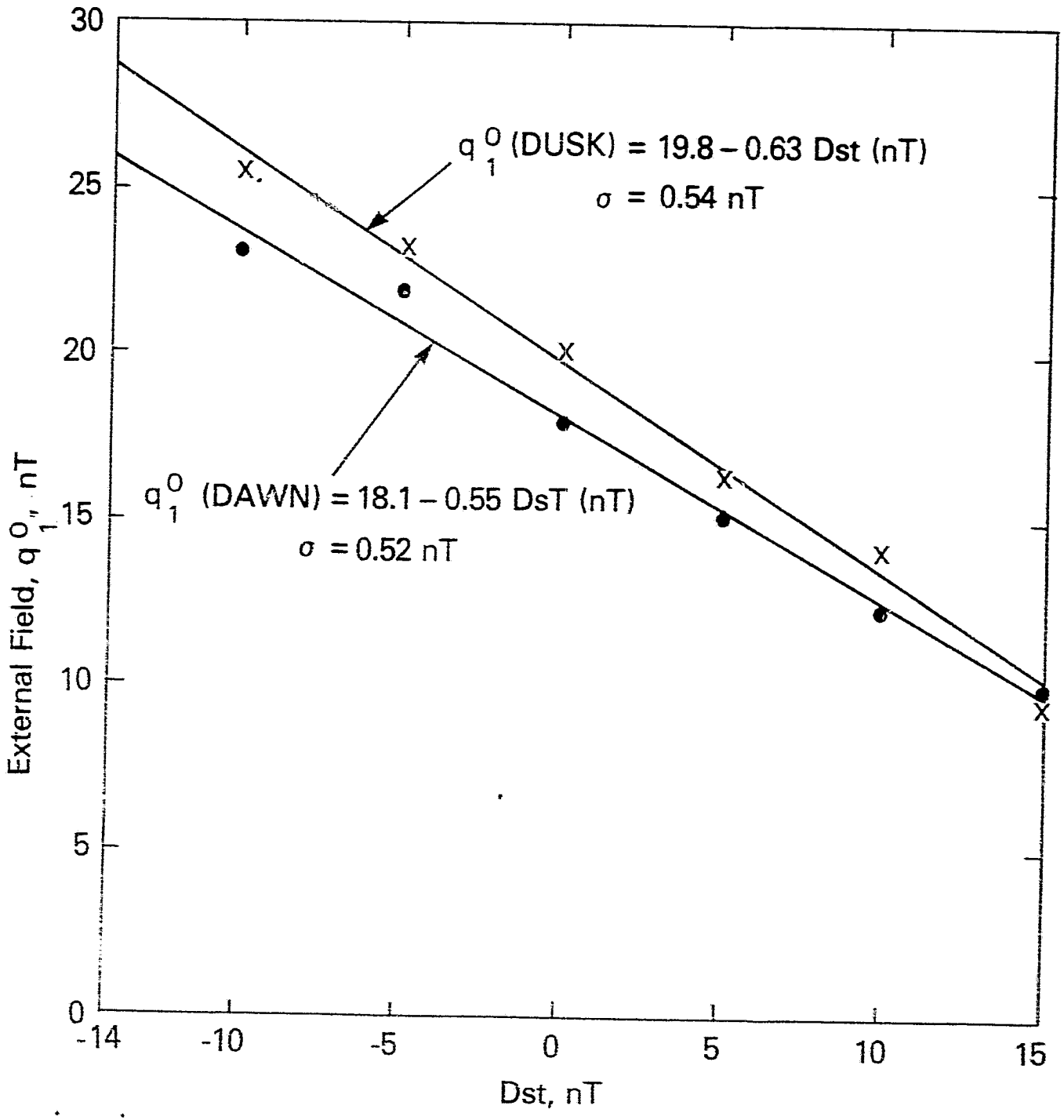
30
25
20
15
10
5
0
-14
-10
-5
0
5
10
15
External Field, q_1^0, nT
Dst, nT
q_1^0 (DUSK) = 19.8 – 0.63 Dst (nT)
σ = 0.54 nT
q_1^0 (DAWN) = 18.1 – 0.55 DsT (nT)
σ = 0.52 nT